16 August 2000

Color Dipole Systematics of the Diffraction Slope in Diffractive Photo- and Electroproduction of Vector Mesons

J. Nemchik

Institute of Experimental Physics, Slovak Academy of Sciences, Watsonova 47, 04353 Košice, Slovakia

Abstract

We present the first evaluation of the color dipole diffraction slope from the data on diffractive photo- and electroproduction of vector mesons. The energy and dipole size dependence of the found dipole diffraction slope are consistent with the color dipole gBFKL dynamics.

Diffractive photo- and electroproduction of vector mesons,

$$\gamma^* p \to V p \quad , \qquad V = \rho^0, \omega^0, \phi^0, J/\Psi, \Upsilon, ... \tag{1}$$

studied within the color dipole model of high energy scattering [1, 2, 3] (see also [4, 5, 6]) offers an unique possibility to scan the color dipole cross section [1, 2, 3, 7], which represents a fundamental quantity and reflects the interaction of the relativistic color dipole of the dipole moment (size) $\mathbf{r}$ with the target nucleon. The alternative description of vector meson production in terms of the gluon structure function of the proton is presented in [8, 9]. Because of the shrinkage of the transverse size of the virtual photon with virtuality Q^2, the vector meson production amplitude scans the color dipole cross section at the dipole size $r \sim r_S$, where the scanning radius r_S can be expressed through the scale parameter A [10, 7]

$$r_S \approx \frac{A}{\sqrt{m_V^2 + Q^2}}\,, \tag{2}$$

where m_V is the vector meson mass and $A \approx 6$. This scanning phenomenon can be also applied for the dipole diffraction slope leading to a decrease of the slope with Q^2 [11, 12] supported by the available experimental data (see below). Detailed analysis of the Q^2 dependence of the Regge growth of the diffration slope for production of charmonium and bottonium states has been presented in the paper [12]. Specifically, the leading twist terms of production amplitudes of the transversely (T) and longitudinally (L) polarized 1S vector mesons in the expansion over the relevant short-distance parameter $r_S^2 \propto 1/(Q^2 + m_V^2)$ are of the form [10, 7]

$$\mathrm{Im}\mathcal{M}_T \propto \frac{1}{Q^2 + m_V^2}\sigma(x_{eff}, r_S) \propto r_S^2 \sigma(x_{eff}, r_S)\,, \tag{3}$$

$$\mathrm{Im}\mathcal{M}_L \approx \frac{\sqrt{Q^2}}{m_V}\mathcal{M}_T \propto \frac{\sqrt{Q^2}}{m_V} r_S^2 \sigma(x_{eff}, r_S)\,. \tag{4}$$

As the result the dipole cross section can be exctracted from the vector meson production cross section. The first evaluation of the dipole cross section from the data on diffractive photo- and electroproduction of vector mesons has been presented in the paper [13]. Following the generalization of the color dipole factorization formula for vector meson production amplitude [1, 2, 3, 14]

$$\mathrm{Im}\mathcal{M}(\gamma^* \to V, x_{eff}, Q^2) = \int\limits_0^1 dz \int d^2\mathbf{r}\sigma(x_{eff}, r)\Psi_V^*(r, z)\Psi_{\gamma^*}(r, z) \tag{5}$$

to the diffraction slope of the reaction $\gamma^* p \to V p$ one can write [12]

$$B(\gamma^* \to V, x_{eff}, Q^2)\mathrm{Im}\mathcal{M}(\gamma^* \to V, x_{eff}, Q^2) = \int\limits_0^1 dz \int d^2\mathbf{r} B(x_{eff}, r)\sigma(x_{eff}, r)\Psi_V^*(r, z)\Psi_{\gamma^*}(r, z)\,, \tag{6}$$

and one can extract also the dipole diffraction slope $B(x_{eff}, r)$ from the vector meson production cross sections using analogical procedure as that for the color dipole cross section extraction published in [13].

In this paper we present the results of the first evaluation of the dipole diffraction slope from the data on real photoproduction and electroproduction of vector mesons (ρ^0, ϕ^0, and J/Ψ) from the fixed target and collider HERA experiments. We find color blindness of the dipole diffraction cone similarly to that for the color dipole cross section. We verify approximate flavor independence of the $B(x_{eff},r)$ in the scaling variable $Q^2+m_V^2$ leading to the close values of the diffraction slope when one takes the same values of the scanning radius. The data from HERA experiments allow also the first evaluation of energy dependence of the dipole diffraction cone at different dipole sizes and confirm the predictions from the BFKL dynamics that a shrinkage with energy of the slope parameter is larger at larger dipole sizes.

We start with the probability amplitudes to find color dipole of size $\mathbf{r}$ in the photon and vector meson. The details of calculation of the diffractive amplitudes have been presented elsewhere [7, 14, 12]. For the $Vq\bar{q}$ vertex function we assume the Lorentz structure $\Gamma\bar{\Psi}\gamma_\mu\Psi V_\mu$. For the s-channel helicity conservation at small $\mathbf{q}$, transverse (T) photons produce the transversely polarized vector mesons and the longitudinally polarized (L) photons (to be more precise, scalar photons) produce longitudinally polarized vector mesons. One finds

$$\mathrm{Im}\mathcal{M}_T(\gamma^*\to V,x_{eff},Q^2)=\frac{N_cC_V\sqrt{4\pi\alpha_{em}}}{(2\pi)^2}\cdot$$
$$\cdot\int d^2\mathbf{r}\sigma(x_{eff},r)\int_0^1\frac{dz}{z(1-z)}\Big\{m_q^2K_0(\varepsilon r)\phi(r,z)-[z^2+(1-z)^2]\varepsilon K_1(\varepsilon r)\partial_r\phi(r,z)\Big\}$$
$$=\frac{C_V}{(m_V^2+Q^2)^2}\int\frac{dr^2}{r^2}\frac{\sigma(x_{eff},r)}{r^2}W_T(Q^2,r^2)$$
$$=g_T\sqrt{4\pi\alpha_{em}}\;C_V\sigma(x_{eff},r_S)\frac{m_V^2}{m_V^2+Q^2} \qquad (7)$$

$$\mathrm{Im}\mathcal{M}_L(\gamma^*\to V,x_{eff},Q^2)=\frac{N_cC_V\sqrt{4\pi\alpha_{em}}}{(2\pi)^2}\frac{2\sqrt{Q^2}}{m_V}\cdot$$
$$\cdot\int d^2\mathbf{r}\sigma(x_{eff},r)\int_0^1 dz\,K_0(\varepsilon r)\Big\{[m_q^2+z(1-z)m_V^2]\phi(r,z)-\partial_r^2\phi(r,z)\Big\}$$
$$=\frac{C_V}{(m_V^2+Q^2)^2}\frac{2\sqrt{Q^2}}{m_V}\int\frac{dr^2}{r^2}\frac{\sigma(x_{eff},r)}{r^2}W_L(Q^2,r^2)$$
$$=g_L\sqrt{4\pi\alpha_{em}}\;C_V\sigma(x_{eff},r_S)\frac{\sqrt{Q^2}}{m_V}\frac{m_V^2}{m_V^2+Q^2} \qquad (8)$$

where

$$\varepsilon^2=m_q^2+z(1-z)Q^2\,, \qquad (9)$$

α_{em} is the fine structure constant, $N_c=3$ is the number of colors, $C_V=\frac{1}{\sqrt{2}},\ \frac{1}{3\sqrt{2}},\ \frac{1}{3},\ \frac{2}{3},\ \frac{1}{3}$ are the charge-isospin factors for the ρ^0, ω^0, ϕ^0, $J/\Psi,\Upsilon$ production, respectively and $K_{0,1}(x)$ are the modified Bessel functions. The detailed discussion and parameterization of the lightcone radial wave function $\phi(r,z)$ of the $q\bar{q}$ Fock state of the vector meson is given in [14]. The terms $\propto K_0(\varepsilon r)\phi(r,z)$ and $\propto\varepsilon K_1(\varepsilon r)\partial_r\phi(r,z)$ for (T), $K_0(\varepsilon r)\partial_r^2\phi(r,z)$ for (L) correspond to the helicity conserving and helicity-flip transitions in the $\gamma^*\to q\bar{q},V\to q\bar{q}$ vertices, respectively.

In (7), (8) the energy dependence of the dipole cross section is quantified in terms of an effective value of the Bjorken variable, x_{eff}, which is connected with dimensionless rapidity, $\xi = \log \frac{1}{x_{eff}}$ and reads

$$x_{eff} = \frac{m_V^2 + Q^2}{2\nu m_p} \sim \frac{Q^2 + m_V^2}{W^2}\,, \tag{10}$$

where m_p and m_V is the proton mass and mass of vector meson, respectively. Hereafter, we will write the energy dependence of the dipole cross section in both variables, either in ξ or in x_{eff}.

Normalization of production amplitudes (7), (8) satisfies the following relation

$$\frac{d\sigma}{dt}|_{t=0} = \frac{|\mathcal{M}|^2}{16\pi} \tag{11}$$

A small real part of production amplitudes can be taken in the form [15]

$$\mathrm{Re}\mathcal{M}(\xi, r) = \frac{\pi}{2} \cdot \frac{\partial}{\partial \xi} \mathrm{Im}\mathcal{M}(\xi, r)\,. \tag{12}$$

and can be easily included in the production amplitudes using substitution

$$\sigma(x_{eff}, r) \to \Big(1 - i\frac{\pi}{2}\frac{\partial}{\partial\ log\ x_{eff}}\Big)\sigma(x_{eff}, r) = \Big[1 - i\alpha_V(x_{eff}, r)\Big]\sigma(x_{eff}, r) \tag{13}$$

Within the mixed $(\mathbf{r}, z)$ representation, the high energy meson is considered as a system of color dipole described by the distribution of the transverse separation $\mathbf{r}$ of the quark and antiquark given by the $q\bar{q}$ wave function, $\Psi(\mathbf{r}, z)$, where z is the fraction of meson's lightcone momentum carried by a quark. The Fock state expansion for the relativistic meson starts with the $q\bar{q}$ state and the higher Fock states $q\bar{q}g$... become very important at high energy ν. The interaction of the relativistic color dipole of the dipole moment, $\mathbf{r}$, with the target nucleon is quantified by the energy dependent color dipole cross section, $\sigma(\xi, r)$, satisfying the gBFKL equation [5, 6] for the energy evolution. This reflects the fact that in the leading-log $\frac{1}{x}$ approximation the effect of higher Fock states can be reabsorbed into the energy dependence of $\sigma(\xi, r)$. The dipole cross section is flavor independent and represents the universal function of r which describes various diffractive processes in unified form. At high energy, when the transverse separation, $\mathbf{r}$, of the quark and antiquark is frozen during the interaction process, the scattering matrix describing the $q\bar{q}$-nucleon interaction becomes diagonal in the mixed $(\mathbf{r}, z)$-representation (z is known also as the Sudakov light cone variable). This diagonalization property is held even when the dipole size, $\mathbf{r}$, is large, i.e. beyond the perturbative region of short distances. Color dipole factorized form of formulas (7), (8) follows from such diagonalization property. The detailed discussion about the space-time pattern of diffractive electroproduction of vector mesons is presented in [14, 12].

Eqs. (7), (8) are related to the pure pomeron exchange, which is important at large values of parameter $\omega = 1/x_{eff}$. However, at moderate and small values of ω there is a substantial contribution to the γN total cross section comming from the non-vacuum Reggeon exchange. The Regge fit to the γp total cross section can be cast in the following form [16]

$$\sigma_{tot} = \sigma_{I\!P}(\gamma p)\Big(1 + \frac{B}{\omega^{\Delta}}\Big) \tag{14}$$

where $B = 2.332$ and $\delta = 0.533$ according to Donnachie-Landshoff fit. In (14) the term B/ω^{Δ} in the factor $f = 1 + B/\omega^{\Delta}$ represents the non-vacuum Reggeon exchange contribution, which is similar also in real ρ^0 photoproduction amplitude. At large Q^2 we assume that the Reggeon/pomeron ratio scales with ω. It is consistent with the known decomposition of the proton structure function into the valence (non-vacuum Reggeon) and sea (pomeron) contributions. Then, for example, at NMC energy $f = 1.25$ at $\omega \sim 70$ relevant to $Q^2 = 3\ GeV^2$ and $f = 1.80$ at $\omega \sim 9$ relevant to $Q^2 = 20\ GeV^2$. At energy attainable at HERA the non-vacuum Reggeon exchange contribution can be neglected because of a large value of the Regge parameter ω. For other vector mesons $(\phi^0, J/\Psi, \Upsilon)$ one expects $f = 1$ due to the Zweig rule. Thus, the forward differential cross section for ρ^0 photo- and electroproduction reads:

$$\frac{d\sigma(\gamma^* \to V)}{dt}|_{t=0} = f^2 \frac{d\sigma_{\mathbb{P}}(\gamma^* \to V)}{dt}|_{t=0} \tag{15}$$

In (7) and (8) we separate out the scanning radius r_S and then the so introduced coefficient functions $g_{T,L}$ are smooth functions of Q^2. Such a procedure is detaily described in the paper [13].

Taking into account the contribution of the real part and the non-vacuum Reggeon exchange to the production amplitude then the experimentally measured forward cross section reads

$$\begin{aligned}\frac{d\sigma(\gamma^* \to V)}{dt}|_{t=0} &= \frac{f^2}{16\pi}\Big[(1+\alpha_{V,T}^2)\mathcal{M}_T^2 + \epsilon(1+\alpha_{V,L}^2)\mathcal{M}_L^2\Big] \\ &= \frac{f^2}{16\pi}(1+\alpha_V^2)\Big[\mathcal{M}_T^2 + \epsilon\mathcal{M}_L^2\Big]\ ,\end{aligned} \tag{16}$$

neglecting the difference between $\alpha_{V,T}$ and $\alpha_{V,L}$ for the transverse and longitudinal cross sections, respectively. Then one can exctract the color dipole cross section from the data on forward production cross section using the above determined coefficient functions g_T and g_L and Eqs. (7), (8), (11) and (16).

$$\begin{aligned}\sigma(x_{eff}, r_S) = \frac{1}{f}\frac{1}{C_V}\frac{Q^2+m_V^2}{m_V^2}\frac{2}{\sqrt{\alpha_{em}}} \\ \times\Big(g_T^2 + \epsilon\frac{Q^2}{m_V^2}g_L^2\Big)^{-1/2}\ (1+\alpha_V^2)^{-1/2}\sqrt{\frac{d\sigma(\gamma^* \to V)}{dt}|_{t=0}}\,,\end{aligned} \tag{17}$$

where ϵ is the longitudinal polarization of the photon. Very often the data are presented in the form of the t- integrated production cross section $\sigma_{tot}(\gamma^* \to V)$. In this case we evaluate

$$\frac{d\sigma(\gamma^* \to V)}{dt}|_{t=0} = B(\gamma* \to V, x_{eff}, Q^2)\sigma_{tot}(\gamma^* \to V) \tag{18}$$

taking the diffraction slope from the same publication.

Now the generalization of the above procedure for extraction of the dipole diffraction slope from the data is following. Comming from the matrix element (6) and taking into account the scanning property one can conclude that the main contribution to the amplidute comes from the dipole size $r_B \sim 5/3\ r_S$ because of r^2 behaviour of the diffraction slope within the color dipole gBFKL dynamics [11, 12]. Then one can introduce another coefficient functions h_T and h_L:

$$B(\gamma^* \to V, x_{eff}, Q^2)\mathcal{M}_T(x_{eff}, Q^2) =$$
$$\frac{C_V}{(m_V^2+Q^2)^2}\int \frac{dr^2}{r^2}\frac{\sigma(x_{eff},r)}{r^2}\frac{B_T(x_{eff},r)}{r^2}\tilde{W}_T(Q^2,r^2) =$$
$$h_T\sqrt{4\pi\alpha_{em}}\; C_V\sigma(x_{eff},r_B)B(x_{eff},r_B)\frac{m_V^2}{m_V^2+Q^2} \tag{19}$$

$$B(\gamma^* \to V, x_{eff}, Q^2)\mathcal{M}_L(x_{eff}, Q^2) =$$
$$\frac{C_V}{(m_V^2+Q^2)^2}\frac{2\sqrt{Q^2}}{m_V}\int \frac{dr^2}{r^2}\frac{\sigma(x_{eff},r)}{r^2}\frac{B_L(x_{eff},r)}{r^2}\tilde{W}_L(Q^2,r^2) =$$
$$h_L\sqrt{4\pi\alpha_{em}}\; C_V\sigma(x_{eff},r_B)B(x_{eff},r_B)\frac{\sqrt{Q^2}}{m_V}\frac{m_V^2}{m_V^2+Q^2} \tag{20}$$

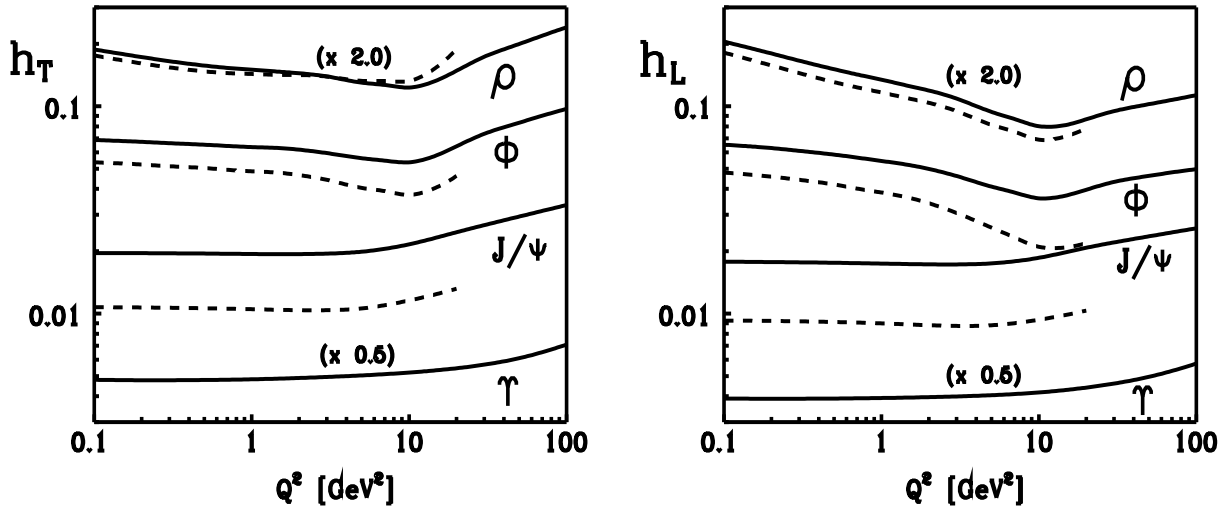

Figure 1: The Q^2 dependence of the coefficient functions $h_{T,L}$ at $W = 15\ GeV$ (dashed curve) and $W = 150\ GeV$ (solid curve).

The possibility of a such relationship between the production amplitude multiplied by the diffraction slope for vector meson production and the dipole cross section multiplied by the dipole diffraction slope at a well defined dipole size $r_B = \frac{5}{3}r_S$ has the same reasons as ones detaily studied and discussed in the paper [13]. In Fig.1 we present the Q^2 dependence of $h_{T,L}$ for different production processes at $W = 15\ GeV$ and $W = 150\ GeV$ reflecting the lower and upper limits of the energy range from the fixed target to HERA experiments. The residual smooth Q^2 behaviour of the coefficient functions $h_{T,L}$ is connected with the smooth and well understood Q^2 dependence of the scale factors $A_{T,L}$, which are presented in the rationship between the scanning radius r_S and the position $A_{T,L}/\sqrt{Q^2+m_V^2}$ of the peak of the functions $\tilde{W}_{T,L}(Q^2,r^2)$. The detailed discussion about the similar smooth Q^2 dependence of the coefficient functions $g_{T,L}$ is presented in [13].

Including the non-vacuum Reggeon contribution and the contribution of the real part to the amplitude (6) the matrix element squared on r.h.s. of Eq. (6) reads:

$$|\mathcal{M}^{\mathcal{B}}(x_{eff},r)|^2 = |<\Psi_V(r,z)|\sigma(x_{eff},r)B(x_{eff},r)|\Psi_{\gamma^*}(r,z)>|^2 =$$

$$f^2(1+\alpha_V^2)4\pi\alpha_{em}C_V^2\frac{m_V^4}{(m_V^2+Q^2)^2}\sigma^2(x_{eff},r_B)B^2(x_{eff},r_B)\Big[h_T^2+\epsilon\frac{Q^2}{m_V^2}h_L^2\Big]= \\ B^2(\gamma^*\to V,x_{eff},Q^2)|_{t=0}\ 16\pi B(\gamma^*\to V,x_{eff},Q^2)\sigma_{tot}(\gamma^*\to V)\ , \qquad (21)$$

where the last line is the l.h.s. squared of Eq. (6) representing the multiplication of the forward diffraction slope squared for vector meson production and vector meson production amplitude squared, which can be expressed via t- integrated production cross section and the diffraction slope using Eqs. (11) and (18).

The experimental determination of the forward diffraction cone $B(t=0)$ requires extrapolation of the differential cross section $d\sigma/dt$ towards $t=0$, which is not always possible and one often reports the t- integrated production cross sections $\sigma_{tot}(\gamma^*\to V)$. Following the high precision $\pi^{\pm}N$ scattering experiments, the diffraction slope $B(t)$ depends strongly on the region of t. For the average $<t>\ \sim 0.1-0.2\ GeV^2$ corresponding usually to the integrated total cross section, the diffraction slope is less than at $t=0$ by $\sim\ 1\ GeV^{-2}$ [17]. Therefore in all cases we report

$$B(\gamma^*\to V,x_{eff},Q^2)|_{t=0}=B(\gamma^*\to V,x_{eff},Q^2)+1\ GeV^{-2}\ , \qquad (22)$$

where $B(x_{eff},Q^2)$ is the diffraction slope determined experimentally from the t- integrated total cross section. Eq. (22) gives an uncertainty $<10\%$ in the value of B and can be reduced if more accurate data will be appeared.

Combining the Eqs. (17), (21) and (22) one can obtain the expression for the dipole diffraction slope $B(x_{eff},r_B)$:

$$B(x_{eff},r_B)=\Big[1+B(\gamma^*\to V,x_{eff},Q^2)\Big]\cdot\sqrt{\frac{g_T^2+\epsilon\frac{Q^2}{m_V^2}g_L^2}{h_T^2+\epsilon\frac{Q^2}{m_V^2}h_L^2}}\cdot\frac{\sigma(x_{eff},r_S)}{\sigma(x_{eff},r_B)}\ , \qquad (23)$$

where $B(\gamma^*\to V,x_{eff},Q^2)$ is the diffraction slope at energy $W\sim\sqrt{\frac{Q^2+m_V^2}{x_{eff}}}$ and at Q^2 taken from the data. In (23) the values of the dipole cross section $\sigma(x_{eff},r_S)$ and $\sigma(x_{eff},r_B)$ are also taken from the same data as the diffraction slope following the procedure of extraction according to Eqs. (17) and (18). In (23) ϵ is the longitudinal polarization of the photon with the values taken from the corresponding experimental publications. One can see from (23) that the dipole diffraction slope is mainly determined by the slope parameter $B(\gamma^*\to V,x_{eff},Q^2)$ obtained from the data, because other two terms in r.h.s. of (23),

$$\sqrt{\frac{g_T^2+\epsilon\frac{Q^2}{m_V^2}g_L^2}{h_T^2+\epsilon\frac{Q^2}{m_V^2}h_L^2}}\quad and\quad \frac{\sigma(x_{eff},r_S)}{\sigma(x_{eff},r_B)}$$

have the residual smooth Q^2 (dipole size) behaviour. It is connected with the smooth Q^2 behaviour of the coefficient functions g_T, g_L, h_T, h_L and with the fact that the ratio of two dipole cross sections at different scanning radii r_S and r_B depends weakly on r_S.

The result of the above described analysis is depicted in Fig.2, which shows the dipole size dependence of the dipole diffraction slope extracted from the low energy and HERA data of photoproduction and electroproduction of vector mesons. The error bars shown here correspond to the error bars in the measured production cross sections and diffraction slopes as cited in the experimental papers. Because the data on vector meson production fall into two broad categories we present the procedure of extraction for two energy ranges:

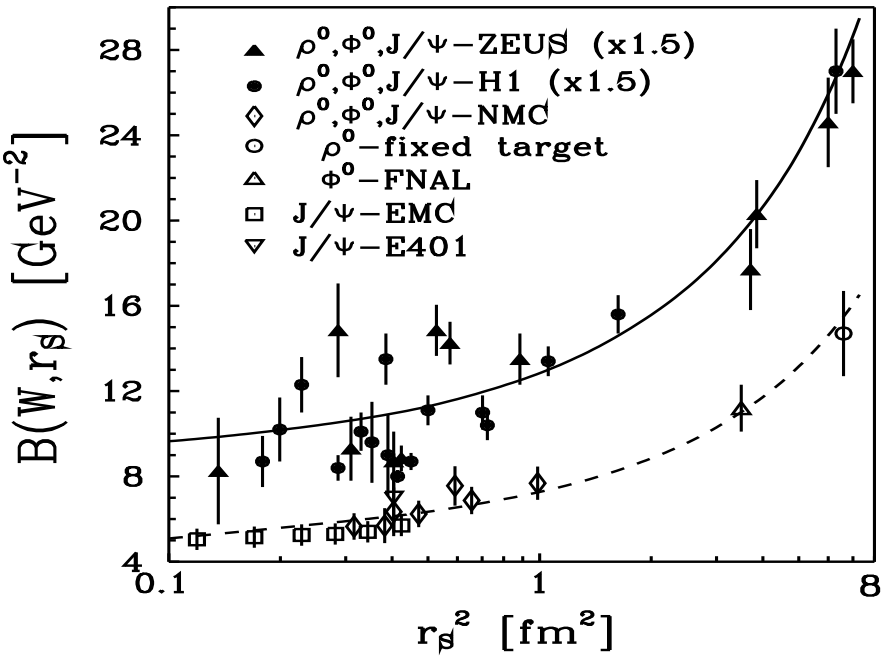

Figure 2: The color dipole size dependence of the dipole diffraction slope extracted from the data on photoproduction and electroproduction of vector mesons: the low energy data on real photoproduction of ρ^0 [18], the low energy data on real photoproduction of Φ^0 [19], the FNAL data on Φ^0 production [20], the NMC data on Φ^0 and ρ^0 production [21], the E401 data on J/Ψ production [22], the EMC data on J/Ψ production [23, 24], the NMC data on J/Ψ production [25], the ZEUS data on ρ^0 production [26, 27, 28, 29, 30, 31], the ZEUS data on Φ^0 production [32], the ZEUS data on J/Ψ production [33, 34], the H1 data on ρ^0 production [35, 36, 37] the H1 data on Φ^0 production [38] and H1 data on J/Ψ production [39, 40, 41, 42, 43]. The dashed and solid curve show the dipole diffraction slope of the model [11, 12] evaluated for the c.m.s. energy $W = 15\ GeV$ and $W = 70\ GeV$, respectively. The data points at HERA energies and the corresponding solid curve are multiplied by the factor 1.5

the center of mass energy $W \sim\ (10 - 15)\ GeV$ corresponding to fixed target data and $W \sim\ (70 - 150)\ GeV$ reflecting the HERA collider data. The color dipole cross section and the color dipole diffraction slope is flavor blind, there is only kinematical dependence on the vector meson through the definition of x_{eff} (see Eq. (10)). However, because of the scanning phenomenon the comparison of reactions with production of different vector mesons at the same value of the scanning radius r_S (at the same value of $Q^2 + m_V^2$) leads approximately to the same corresponding values of x_{eff} at the fixed energy ν. Thus, one expect that the extraction procedure (23), (17) applied to the different vector mesons will lead to the same value of $B(x_{eff}, r_S)$ at the same value of the scanning radius. This situation is similar to that for the color dipole cross section. Again, the data show the decrease of the dipole diffraction cone towards small dipole size r_S. It reflexes the contribution of the geometrical term $\propto r^2$ to the diffraction slope [11, 12]. A comparison of the low energy fixed-target and HERA data on real photoproduction and electroproduction of vector mesons is not in contradiction

with the conclusion about a substantial shrinkage of the dipole diffraction cone coming from the gBFKL phenomenology [11, 12]. The corresponding effective shrinkage rate α'_{eff} for ρ^0 photoproduction is about 0.25 GeV^{-2} at the energy range of fixed target experiments and slightly decreases to the value of about 0.2 GeV^{-2} at HERA energy. For electroproduction of charmonium and electroproduction of ρ^0 when the scanning radius $\sim 0.2 - 0.3$ fm, the corresponding $\alpha'_{eff} \sim 0.15\ GeV^{-2}$ at HERA energies in accordance with the gBFKL phenomenology of a subasymptotic energy dependence of the diffraction slope [11, 12]. In another words, the shrinkage of the diffraction slope with energy is weaker at smaller dipole sizes. However, large error bars of the diffraction slope data does not allow to see clearly the shrinkage of the slope parameter with energy. Some evidence of that shrinkage is seen only at large dipole sizes $r_S \gtrsim 1$ fm, where the rise with energy of the slope is predicted to be more substantial.

The above determination of the color dipole diffraction slope from the data is rather crude for the following reasons reported particularly in the paper [13]:
i) The vector meson production data from the EMC collaboration is known to have been plagued by a background from the inelastic process $\gamma^* p \to VX$. Especially at large Q^2 it could lead to enhancement of the production cross section whereas the diffraction slope could have been underestimated. In the recent NMC data [21] a special care has been taken to eliminate an inelastic background and the values of $B(x_{eff}, r_S)$ from the NMC data are consistent within the experimental error bars.
ii) There are uncertainties connected with extrapolation of the differential cross section down to $t = 0$. Due to the curvature of the diffraction cone the forward production cross section can be underestimated.
iii) There is also conservative $\lesssim 15\%$ theoretical inaccuracy of the extraction procedure connected with the variation of the coefficient functions g_T, g_L, h_T and h_L as a function of Q^2 from small ($W = 15\ GeV$) to large ($W = 150\ GeV$) energy (see also paper [13]).
iiii) There is residual uncertainty connected with the wave function of light vector mesons.

To summarize, within the above stated uncertainties of the simple extraction procedure and the experimental errors bars, there is a consistency between the dipole diffraction slope determined from ρ^0, Φ^0 and J/Ψ production data. This is the first direct determination of the dipole diffraction slope and the main conclusions are not affected by the above cited uncertainties.

Fig.2 shows also the dipole diffraction slope from the gBFKL analysis [11, 12], which gives an unified description of the data on vector meson diffractive production and on the proton structure function.

Conclusions.

We present the first determination of the dipole diffraction slope from the data on diffractive photo- and electroproduction of vector mesons. The dipole diffraction slope has been evaluated at the dipole size down to $r_S \sim 0.35$ fm and the decrease of $B(x_{eff}, r_S)$ towards small r_S is in accordance with r_S^2 behaviour of the diffraction slope coming from the gBFKL phenomenology. Because of large error bars of the data, we found only an evidence of a shrinkage of $B(x_{eff}, r_S)$ with energy from the fixed-target, $W \sim 10 - 15\ GeV$ up to collider HERA energy range, $W \sim 70 - 150\ GeV$. This shrinkage is weaker for smaller dipole sizes. The found pattern of dipole size and energy dependence of the dipole diffraction slope is consistent with the flavor independence and with expectations from the gBFKL dynamics.

References

[1] B.Z.Kopeliovich and B.G.Zakharov, *Phys. Rev.* **D44** (1991) 3466.

[2] N.N.Nikolaev, *Comments on Nucl. Part. Phys.* **21** (1992) 41.

[3] B.Z.Kopeliovich, J.Nemchik, N.N.Nikolaev and B.G.Zakharov, *Phys. Lett.* **B309** (1993) 179.

[4] N.N. Nikolaev and B.G. Zakharov, *Z. Phys.* **C49** (1991) 607; *Z. Phys.* **C53** (1992) 331.

[5] N.Nikolaev and B.G.Zakharov, *JETP* **78** (1994) 598; *Z. Phys.* **C64** (1994)631.

[6] N.N.Nikolaev, B.G.Zakharov and V.R.Zoller, *JETP Letters* **59** (1994) 6; *JETP* **78** (1994) 866; *Phys. Lett.* **B328** (1994) 486.

[7] J.Nemchik, N.N.Nikolaev and B.G.Zakharov, *Phys. Lett.* **B341** (1994) 228.

[8] M.G.Ryskin, *Z. Phys.* **C57** (1993) 89.

[9] S.J.Brodsky et al., *Phys. Rev.* **D50** (1994) 3134.

[10] B.Z.Kopeliovich, J.Nemchik, N.N.Nikolaev and B.G.Zakharov, *Phys. Lett.* **B324** (1994) 469.

[11] N.N.Nikolaev, B.G.Zakharov and V.R.Zoller, *Phys. Lett.* **B366** (1996) 337

[12] J.Nemchik, N.N.Nikolaev, E.Predazzi, B.G.Zakharov and V.R.Zoller, *JETP* **86** (1998) 1054.

[13] J.Nemchik, N.N.Nikolaev, E.Predazzi and B.G.Zakharov, *Phys. Lett.* **B374** (1996) 199.

[14] J.Nemchik, N.N.Nikolaev, E.Predazzi and B.G.Zakharov, *Z. Phys* **C75** (1997) 71.

[15] V.N.Gribov and A.A.Migdal, *Sov. J. Nucl. Phys.* **8** (1969) 703.

[16] A.Donnachie and P.V.Landshoff, *Phys. Lett.* **B296** (1992) 227,
Phys. Lett. **B348** (1995) 213.

[17] A.Schiz, L.A.Fajardo, R.Majka et al., *Phys. Rev.* **D24** (1981) 26.
J.P.Burq, M.Chemarin, M.Chevallier et al., *Phys. Lett.* **B109** (1982) 111.

[18] W.G.Jones et al., *Phys. Rev. Lett.* **21** (1968) 586;
C.Berger et al., *Phys. Lett.* **B39** (1972) 659;
SBT Collab., J.Ballam et al., *Phys. Rev.* **D5** (1972) 545;
J.Park et al. *Nucl. Phys.* **B36** (1972) 404;
G.E.Gladding et al., *Phys. Rev.* **D8** (1973) 3721;
R.M.Egloff et al. *Phys. Rev. Lett.* **43** (1979) 657;
OMEGA Collab., D.Aston et al. *Nucl. Phys.* **B209** (1982) 56.

[19] R.Erbe et al., *Phys. Rev.* **175** (1968) 1669;
C.Berger et al., *Phys. Lett.* **B39** (1972) 659;
J.Ballam et al., *Phys. Rev.* **D7** (1973) 3150;
H.J.Bersh et al., *Nucl. Phys.* **B70** (1974) 257;
H.J.Behrend et al., *Phys. Lett.* **B56** (1975) 408;
D.P.Barber et al., *Phys. Lett.* **B79** (1978) 150;
D.Aston et al., *Nucl. Phys.* **B172** (1980) 1;
M.Atkinson et al., *Z. Phys.* **C27** (1985) 233.

[20] J. Busenitz et al., *Phys. Rev.* **D40** (1989) 40 and references therein.

[21] NMC Collab., M.Arneodo, et al., *Nucl. Phys.* **B 429** (1994) 503.

[22] E401 Collab., M.Binkley et al., *Phys. Rev. Lett.* **48** (1982) 73.

[23] EMC Collab., J.J.Aubert et al., *Phys. Lett.* **B89** (1980) 267.

[24] EMC Collab., J.J.Aubert et al., *Nucl. Phys.* **B213** (1983) 1;
J.Ashman et al.,*Z. Phys.* **C39** (1988) 169.

[25] NMC Collab., M.Arneodo, et al., *Phys. Lett.* **B 332** (1994) 195.

[26] ZEUS Collab., M.Derrick et al., *Z. Phys.* **C63** (1994) 391.

[27] ZEUS Collab., M.Derrick et al., *Z. Phys.* **C69** (1995) 39.

[28] ZEUS Collab., M.Derrick et al., *Phys. lett.* **B356** (1995) 601.

[29] ZEUS Collab., M.Derrick et al., *Z. Phys.* **C73** (1997) 253.

[30] ZEUS Collab., J.Breitweg et al., *Eur. Phys. J.* **C2** (1998) 247.

[31] ZEUS Collab., J.Breitweg et al., *Eur. Phys. J.* **C6** (1999) 603.

[32] ZEUS Collab., M.Derrick et al., *Phys. Lett.* **B377** (1996) 259.

[33] ZEUS Collab., M.Derrick et al., *Phys. Lett.* **B350** (1995) 120.

[34] ZEUS Collab., J.Breitweg et al., *Z. Phys.* **C75** (1997) 215.

[35] H1 Collab., S.Aid et al., *Nucl. Phys.* **B463** (1996) 3.

[36] H1 Collab., S.Aid et al., *Nucl. Phys.* **B468** (1996) 3.

[37] H1 Collab., C.Adloff et al., *Eur. Phys. J.* **C13** (2000) 371.

[38] H1 Collab., C.Adloff et al., *Z. Phys.* **C75** (1997) 607.

[39] H1 Collab., T.Ahmed et al., *Phys. Lett.* **B338** (1994) 507.

[40] H1 Collab., S.Aid et al.,*Nucl. Phys.* **B468** (1996) 3.

[41] H1 Collab., S.Aid et al.,*Nucl. Phys.* **B472** (1996) 3.

[42] H1 Collab., C.Adloff et al.,*Eur. Phys. J.* **C10** (1999) 373.

[43] H1 Collab., C.Adloff et al.,*DESY preprint* **DESY-00-037** (1999) DESY, submitted to *Phys. Lett.* **B**